MATHEMATICAL MODELING AND COMPUTING, Vol. 10, No. 2, pp. 261–271 (2023)

Dynamical behavior of predator–prey model with non-smooth prey harvesting

Meziani T., Mohdeb N.

Applied Mathematics Laboratory, Faculty of Exact Sciences, University of Bejaia, Algeria

(Received 11 July 2022; Revised 22 January 2023; Accepted 27 January 2023)

The objective of the current paper is to investigate the dynamics of a new predator–prey model, where the prey species obeys the law of logistic growth and is subjected to a non-smooth switched harvest: when the density of the prey is below a switched value, the harvest has a linear rate. Otherwise, the harvesting rate is constant. The equilibria of the proposed system are described, and the boundedness of its solutions is examined. We discuss the existence of periodic solutions; we show the appearance of two limit cycles, an unstable inner limit cycle and a stable outer one. As the values of the model parameters vary, several kinds of bifurcation for the model are detected, such as transcritical, saddle–node, and Hopf bifurcations. Finally, some numerical examples of the model are performed to confirm the theoretical results obtained.

Keywords: *predator–prey model; switched harvest; stability; bifurcation; limit cycle.*

2010 MSC: 34A34, 34C23, 34C25, 34C45, 34D23 **DOI:** 10.23939/mmc2023.02.261

1. Introduction

Predator–prey systems have long been and will continue to be one of the most important population models that have received extensive attention in both environmental and mathematical ecology [1]. Since the advent of the historic Lotka–Volterra model, this field has attracted many researchers who not only improved their models but also studied and added many more aspects affecting the dynamics of populations [2–12] and wanted to know what models can best represent species interactions.

Different types of predator–prey systems exist that model the dynamics of populations in which two species interact. In the simplest form, the interaction between predators and preys can be modeled by the following differential system with logistic growth of prey [13]

$$\begin{cases} \dot{x} = rx\left(1 - \dfrac{x}{k}\right) - axy, \\ \dot{y} = y(-d + cx), \end{cases} \tag{1}$$

where $x(t)$ and $y(t)$ represent the densities of the prey and predator species at time t, respectively. The parameters r, k, a, c and d are all positive constants. The variable r is the intrinsic growth rate of the prey without predation and carrying capacity k. The amount of prey consumed by a predator per unit of time is given by ax, where a denotes the rate of predation. The factor c indicates the predator's growth rate due to its predation and d represents the natural death rate of the predator. The dynamical behavior of the model (1) is well-known and relatively simple: as $k < \frac{d}{c}$, the boundary equilibrium $(k, 0)$ with the predator going extinct, is globally asymptotically stable, and no positive equilibrium exists for the prey-predator interaction. As $k > \frac{d}{c}$, the boundary equilibrium $(k, 0)$ is an unstable saddle point, and there exists a positive coexistence equilibrium $(\frac{d}{c}, \frac{r}{a}(1 - \frac{d}{ck}))$, which is globally asymptotically stable. Using k as a bifurcation value, a transcritical bifurcation occurs at $k = \frac{d}{c}$. Notice that model (1) has no limit cycle.

To enrich the model (1), many researchers modify the nonlinear functional response and add some other elements such as: toxicity [14], pollution [15], the Allee effect [16], refuge [17], etc. As harvesting is an important and effective method to prevent and control the explosive growth of predators or preys when they are enough, it is reasonable and necessary to introduce the harvest of populations into models.

Several forms of harvesting in predator–prey models have been widely studied. Researchers have added the harvest to the prey component [4, 10, 18] or to the predator [5, 8, 11, 19] or to both species simultaneously [20–22]. The most common one of these harvesting forms is a nonzero constant or a linear harvesting rate. Many authors have studied the problem of predator–prey interactions under the constant or linear rate of harvesting of either species or both species simultaneously: Xiao and Jennings [10], Xiao et al. [11] have studied the dynamics of ratio-dependent predator-prey models with constant harvesting rates. Vijayalakshmi and Senthamarai [22], Xiao and Cao [9], Y. Zhang and Q. Zhang [12], have investigated a predator–prey model with a linear harvesting rate. Models studied with linear or constant harvesting rates exhibit far richer and more complex dynamics compared to the models with no harvesting. Moreover, the two kinds of harvesting rates have their own advantages as well as disadvantages in the dynamic evolution of a population that is subject to it. Bing Li et al. [6] have studied a new predator-prey model with non-smooth switched harvest on the predator. They have constructed a new type of harvesting rate that combines the advantages of both linear and constant harvesting rates. Their model presents new dynamical features compared to those with a linear harvesting rate or a constant harvesting rate; they have obtained interesting results, such as the existence and stability of multiple equilibria, the existence of two limit cycles and the appearance of various bifurcations.

Motivated by the idea used in [6], in the present paper, we propose a predator–prey model (1) with non-smooth switched harvest on the prey, we assume that the predator in the model (1) is not of commercial importance and the prey is continuously being harvested at a linear harvesting rate if his density is below a switched value, and at a constant harvesting rate, otherwise. We show that this model has rich dynamics.

This paper is organized as follows: in Section 2, we present the mathematical model formulation. In Section 3, we give some basic results; we prove that the solutions of the system are bounded, which, in turn, implies that the system is biologically well-behaved. Furthermore, we explore the dynamics of the proposed model by examining the existence and the stability of the equilibrium points. We show the existence of limit cycles, and we analyze different bifurcations. In Section 4, we present some numerical examples to illustrate and confirm the established results. A brief discussion about the obtained results is given finally in Section 5.

2. Model formulation

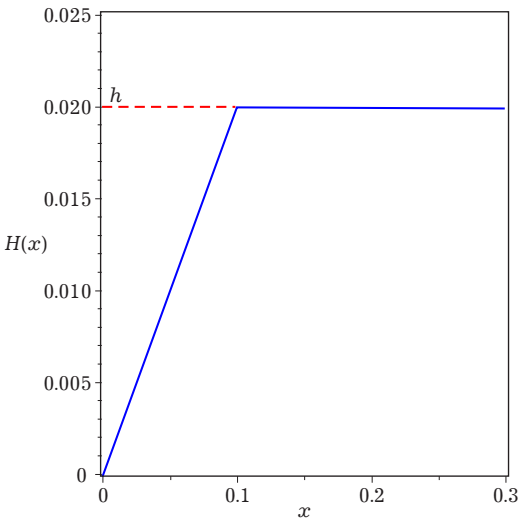

Fig. 1. Harvesting function for $\bar{x} = 0.1$, $m = 0.2$, and $h = 0.02$.

In this section, we aim to develop the predator–prey model (1) by introducing the following harvesting function $H(x)$ on the prey component,

$$H(x) = \begin{cases} mx & \text{if} \quad 0 \leqslant x \leqslant \bar{x}, \\ h & \text{if} \quad x > \bar{x}, \end{cases} \tag{2}$$

where m and $\bar{x}$ are positive real numbers such that, m represents the rate of harvesting, $\bar{x}$ is the threshold value and $h = m\bar{x}$ denotes the harvesting threshold value.

We assume that the harvesting rate is proportional to the prey population size until it reaches a threshold value due to limited facilities of harvesting or resource protection. The harvesting rate will then be kept as a constant.

We implement the harvesting function (2) in a predator–prey model (1), we obtain the following system

$$\begin{cases} \dot{x} = rx\left(1 - \dfrac{x}{k}\right) - axy - H(x), \\ \dot{y} = y(-d + cx). \end{cases} \tag{3}$$

Model (3), when $0 \leqslant x \leqslant \bar{x}$, is

$$\begin{cases} \dot{x} = rx\left(1 - \dfrac{x}{k}\right) - axy - mx, \\ \dot{y} = y(-d + cx), \end{cases} \tag{4}$$

and when $x > \bar{x}$, is

$$\begin{cases} \dot{x} = rx\left(1 - \dfrac{x}{k}\right) - axy - h, \\ \dot{y} = y(-d + cx). \end{cases} \tag{5}$$

3. Mathematical analysis and main results

The main concern of this paper is to study the dynamical behaviors of predator–prey model (3); for biological considerations, we are only interested in the dynamics of model (3) in the first quadrant $\mathbb{R}^2_+$, we consider only the biologically meaningful initial conditions, $x(0) \geqslant 0$ and $y(0) \geqslant 0$.

3.1. Boundedness of solutions of (3)

First, we show that all solutions of (3) starting in $\mathbb{R}^2_+$ are bounded.

Theorem 1. *All solutions of system* (3) *with positive initial conditions are positive for all* $t \geqslant 0$ *and ultimately bounded, and the set*

$$S = \left\{(x, y) \in \mathbb{R}^2_+,\ cx + ay \leqslant \frac{ck}{4rd}(r + d)^2\right\}$$

is positive invariant for system (3).

Proof. For positive initial conditions $(x_0, y_0) = (x(0), y(0))$, it is easy to see that $x(t) > 0$ and $y(t) > 0$ for all $t \geqslant 0$.

Let $\omega(t) = cx(t) + ay(t)$. For each $\zeta > 0$, we have

$$\dot{\omega} + \zeta\omega \leqslant \frac{ck}{4r}(r + \zeta)^2 - y(a(d - \zeta)). \tag{6}$$

If we choose $\zeta \leqslant d$, then right hand side of (6) is bounded for all $(x, y) \in \mathbb{R}^2_+$. Thus we have $\dot{\omega} + \zeta\omega \leqslant \mu$, where $\mu = \frac{ck}{4r}(r + d)^2 > 0$.

Applying the theory of differential inequality [23], we get

$$0 < \omega(t) \leqslant \frac{\mu}{\zeta}\left(1 - e^{-\zeta t}\right) + \omega(0)e^{-\zeta t}.$$

We show that

$$\frac{\mu}{\zeta}\left(1 - e^{-\zeta t}\right) + \omega(0)e^{-\zeta t} \leqslant \max\left\{\frac{\mu}{\zeta}, \omega(0)\right\}. \tag{7}$$

If (x_0, y_0) is in S, then $\omega(0) \leqslant \frac{\mu}{\zeta}$, and by (7), $\omega(t) \leqslant \frac{\mu}{\zeta}$ for all $t \geqslant 0$.

Therefore, $(x(t), y(t)) \in S$, $\forall t \geqslant 0$. ∎

3.2. Equilibria and their stability

In this part, we determine the equilibria of system (3) and their stability in the quadrant $\mathbb{R}^2_+$. We can see that there exists a non-negative equilibrium of system (3) if and only if the equations

$$\begin{cases} rx\left(1 - \dfrac{x}{k}\right) - axy - H(x) = 0, \\ y(-d + cx) = 0 \end{cases} \tag{8}$$

have a pair of non-negative real solutions (x, y).

3.2.1. Equilibrium points for $0 \leqslant x \leqslant \bar{x}$

Proposition 1. When the number of preys is less than the threshold value, the system (3) has three equilibria:

1) $p_0 = (0, 0)$;
2) $p_1 = (k(1 - \frac{m}{r}), 0)$;
3) $p^* = (x^*, y^*)$;

where $x^* = \frac{d}{c}$ and $y^* = \frac{r}{a}(1 - \frac{d}{ck}) - \frac{m}{a}$.

Their existence in the first quadrant $\mathbb{R}^2_+$, for $0 \leqslant x \leqslant \bar{x}$ depends on the following conditions:

i) if $r\left(1 - \frac{\bar{x}}{k}\right) \leqslant m < r$, p_1 lies in $\mathbb{R}^2_+$;
ii) if $m < r\left(1 - \frac{d}{ck}\right)$ and $\frac{d}{c} \leqslant \bar{x}$, p^* lies in $\mathbb{R}^2_+$.

The equilibrium p_0 represents the extinction of both predator and prey species, which always exists. The equilibrium p_1 indicates the persistence of the prey population in the absence of predator population and the equilibrium p^* represents the coexistence of both prey and predator species.

Now, we study the dynamics of system (3) in the neighborhood of each equilibrium. When $0 \leqslant x \leqslant \bar{x}$, the dynamics of system (3) in the neighborhood of an equilibrium comes directly from the property of eigenvalues of the Jacobian matrix

$$\mathfrak{J}_1(x, y) = \begin{pmatrix} r(1 - \frac{2x}{k}) - ay - m & -ax \\ cy & -d + cx \end{pmatrix}.$$

Proposition 2. In system (3):

1) p_0 is an unstable saddle point, when $m < r$;
2) p_0 is a stable node, when $m > r$;
3) p_1 is an unstable saddle point, when $m < r(1 - \frac{d}{ck})$;
4) p_1 is a stable node, when $m > r(1 - \frac{d}{ck})$.

Remark 1. When $m = r(1 - \frac{d}{ck})$, we will show that there exists a bifurcation at p_1, depending on further conditions discussed in subsection 3.4.

The analysis of the stability of $p^* = (\frac{d}{c}, \frac{r}{a}(1 - \frac{d}{ck}) - \frac{m}{a})$ can be accomplished by analyzing the trace-determinant plane $(\tau_1, \mathcal{D}_1)$ of its Jacobian, where

$$\tau_1 = -\frac{dr}{ck} < 0 \quad \text{and} \quad \mathcal{D}_1 = acx^*y^*.$$

The positive equilibrium p^* exists in $\mathbb{R}^2_+$ if and only if $m < r(1 - \frac{d}{ck})$ and $\frac{d}{c} < \bar{x}$, therefore $\mathcal{D}_1 > 0$. Thus all eigenvalues of matrix $\mathfrak{J}_1(p^*)$ have negative real parts. It follows that p^* is locally asymptotically stable. Moreover, we have the following result.

Theorem 2. *The positive equilibrium p^* of system (3) is globally asymptotically stable.*

Proof. We show the global stability of $p^* = (x^*, y^*)$ by constructing a suitable Lyapunov function

$$\mathcal{V}(t) = cx^* \left(\frac{x(t)}{x^*} - \log \frac{x(t)}{x^*} - 1 \right) + ay^* \left(\frac{y(t)}{y^*} - \log \frac{y(t)}{y^*} - 1 \right).$$

it can be easily verified that the function $\mathcal{V}$ is zero at the equilibrium point (x^*, y^*), and is positive for all other positive values of x and y, thus $\mathcal{V}$ is positive definite.

The time derivative along the trajectories of system (3) is,

$$\begin{aligned} \frac{d\mathcal{V}(t)}{dt} &= c\left(1 - \frac{x^*}{x}\right)\frac{dx}{dt} + a\left(1 - \frac{y^*}{y}\right)\frac{dy}{dt} \\ &= -\frac{rc}{k}\left(x - \frac{d}{c}\right)^2. \end{aligned}$$

Clearly $\frac{d\mathcal{V}(t)}{dt} \leqslant 0$ for all $t \geqslant 0$, thus it is negative semi-definite. Furthermore, it can be verified that $\frac{d\mathcal{V}(t)}{dt}$ is zero if and only if $x = x^*$, and by the first equation of system (4), we get $y = y^*$. By the LaSalle invariance principle [24], all the solutions starting in $\mathbb{R}^2_+$ approach the equilibrium point p^*, and it is globally asymptotically stable. ∎

3.2.2. Equilibrium points when $x > \bar{x}$

When the number of preys is above the threshold value, the system (3) has at most three equilibria. Therefore, we have the following proposition which describes the number and location of equilibria of system (3), when $x > \bar{x}$. We define

$$h_1 = \frac{rk}{4}, \quad h_2 = \frac{rd}{c}\left(1 - \frac{d}{ck}\right), \quad h_3 = r\bar{x}\left(1 - \frac{\bar{x}}{k}\right), \quad \hat{h} = \frac{rd^2}{kc^2}.$$

Proposition 3. Assume $\bar{x} < \frac{k}{2}$. System (3) in the first quadrant $\mathbb{R}^2_+$ with $x > \bar{x}$, has:

1) no positive equilibrium, if $h > h_1$;
2) a unique equilibrium, $q_0 = (\frac{k}{2}, 0)$, if $h = h_1$;
3) two equilibria, $q_1 = (x_1', 0)$ and $q_2 = (x_2', 0)$ with $x_1' = \frac{rk - \sqrt{rk(rk-4h)}}{2r}$ and $x_2' = \frac{rk + \sqrt{rk(rk-4h)}}{2r}$, if $h_2 < h < h_1$ and $h > h_3$;
4) three equilibria, $q_1 = (x_1', 0)$, $q_2 = (x_2', 0)$ and $q^* = (\hat{x}, \hat{y})$ with $\hat{x} = \frac{d}{c}$ and $\hat{y} = \frac{r}{a}\left(1 - \frac{d}{ck}\right) - \frac{ch}{ad}$, if $h < h_1$, $\frac{d}{c} > \bar{x}$ and $h_3 < h < h_2$.

Now, we study the stability properties of the equilibria q_0, q_1, q_2 and q^*.

The Jacobian matrix of system (3) for $x > \bar{x}$, is given by

$$\mathfrak{J}_2(x, y) = \begin{pmatrix} r(1 - \frac{2x}{k}) - ay & -ax \\ cy & -d + cx \end{pmatrix}.$$

The equilibrium point q_0 is nonhyperbolic and we have the following theorem.

Theorem 3. *The equilibrium q_0 is: (1) a saddle-node if $-d + \frac{ck}{2} \neq 0$, (2) a saddle if $-d + \frac{ck}{2} = 0$.*

Proof. The two eigenvalues of the Jacobian $\mathfrak{J}_2(q_0)$ are: $\lambda_1 = 0$ and $\lambda_2 = -d + \frac{ck}{2}$. To determine the dynamics of system (3) in the neighborhood of the equilibrium $q_0 = (\frac{k}{2}, 0)$, we first translate the equilibrium $q_0 = (\frac{k}{2}, 0)$ of system (3) to the origin. Then system (3) becomes

$$\begin{cases} \dot{X} = -\frac{ak}{2}Y - aXY - \frac{r}{k}X^2, \\ \dot{Y} = \left(-d + \frac{ck}{2}\right)Y + cXY, \end{cases} \tag{9}$$

where $X = x - \frac{k}{2}$ and $Y = y$.

First, if $-d + \frac{ck}{2} \neq 0$, then there exists a smooth nonsingular transformation

$$\begin{cases} u = X + \frac{ak}{ck - 2d}Y, \\ v = Y \end{cases}$$

such that system (9) becomes

$$\begin{cases} \dot{u} = A_1(u, v), \\ \dot{v} = \lambda v + B_1(u, v), \end{cases} \tag{10}$$

where $\lambda = -d + \frac{ck}{2}$, $A_1(u, v) = -\frac{r}{k}u^2 - \left(\frac{a^2k}{2\lambda} + \frac{rka^2}{4\lambda^2} - \frac{a^2k^2c}{4\lambda^2}\right)v^2 + \left(\frac{ar}{\lambda} + \frac{ack}{2\lambda} - a\right)uv$ and $B_1(u, v) = cuv - \frac{ack}{2\lambda}v^2$ are analytic functions in a neighborhood of $(0, 0)$. From straightforward analysis of system (10), the equilibrium $(0, 0)$ of (10) is a saddle-node by [25] (Theorem 2.19, chapter 2). This implies the equilibrium $q_0 = (\frac{k}{2}, 0)$ of system (3) is a saddle-node (Figure 2*a* and 2*c*).

If $-d + \frac{ck}{2} = 0$, then both eigenvalues of the matrix $\mathfrak{J}_2(q_0)$ are zero. Note that the matrix $\mathfrak{J}_2(q_0)$ is not zero matrix. Thus, system (9) can be transformed to

$$\begin{cases} \dot{u} = v + A_2(u, v), \\ \dot{v} = B_2(u, v), \end{cases} \tag{11}$$

where $A_2(u, v) = \frac{2}{k}uv + \frac{2r}{ak^2}u^2$ and $B_2(u, v) = \frac{-2c}{ak}uv$ are analytic functions in a neighborhood of $(0, 0)$. From [25] (Theorem 3.5, chapter 3), the equilibrium $(0, 0)$ of system (11) is a saddle. This implies the equilibrium $q_0 = (\frac{k}{2}, 0)$ of system (3) is a saddle (Figure 2*b*). ∎

By looking for the characteristic roots to the linearized equation of (3), at equlibria q_1 and q_2, we get the following result.

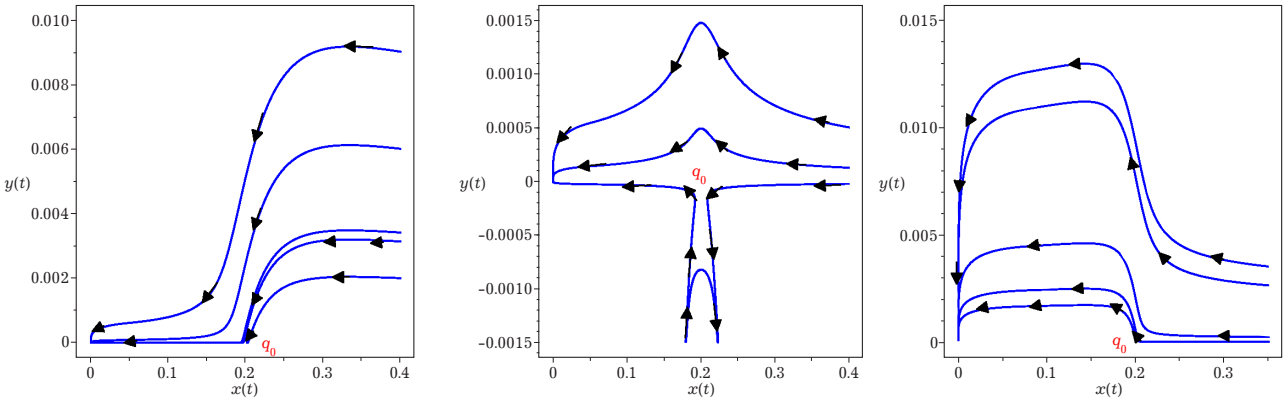

a ***b*** ***c***

Fig. 2. The phase portrait of system (3) with equilibrium q_0: (***a***) $\frac{ck}{2} - d < 0$; (***b***) $\frac{ck}{2} - d = 0$; (***c***) $\frac{ck}{2} - d > 0$.

Proposition 4. The equilibrium q_1 is:

(1) an unstable node, if $h > h_2$ and $\frac{d}{c} < \frac{k}{2}$; (2) a saddle point, if $h > h_2$ and $\frac{d}{c} > \frac{k}{2}$ or if $h < h_2$.

The equilibrium q_2 is:

(3) a stable node, if $h > h_2$ and $\frac{d}{c} > \frac{k}{2}$; (4) a saddle point, if $h > h_2$ and $\frac{d}{c} < \frac{k}{2}$ or if $h < h_2$.

Now, we investigate the stability of the equilibrium $q^* = (\frac{d}{c}, \frac{r}{a}\left(1 - \frac{d}{ck}\right) - \frac{ch}{ad})$. The trace (τ_2) and the determinant $(\mathcal{D}_2)$ of the Jacobian $\mathfrak{J}_2(q^*)$, are

$$\tau_2 = \frac{hc}{d} - \frac{rd}{ck} \quad \text{and} \quad \mathcal{D}_2 = dr\left(1 - \frac{d}{ck}\right) - hc.$$

The analysis of the stability of q^* can be accomplished by analyzing the trace-determinant plane. The positive equilibrium q^* exists in $\mathbb{R}^2_+$ if and only if $h < \min\{h_1, h_2\}$, therefore $\mathcal{D}_2 > 0$. Then we have the following.

Proposition 5. The positive equilibrium q^* of system (3) is,

1) an unstable focus or node if $h > \hat{h}$;
2) a weak focus if $h = \hat{h}$;
3) asymptotically stable if $h < \hat{h}$.

3.3. Existence of limit cycles

Since the existence of limit cycles in dynamical systems plays an important role in determining the dynamical behavior of solutions, we explore in this part the existence of limit cycles in system (3).

Theorem 4. *Suppose $\hat{h} < h < \min\{h_1, h_2\}$. If $m < r$, then system (3) has at least a stable limit cycle.*

Proof. For $\hat{h} < h < \min\{h_1, h_2\}$, the equilibrium q^* exists and it is an unstable focus or node. Furthermore, if $h < h_2$, the equilibrium q_2 is an unstable saddle point and if $m < r$, the origin p_0 is a saddle point. Then there are two separatrices of saddle p_0 and q_2 tends to a movement periodic.

As the set S is positively invariant for system (3), and system (3) does not have any equilibrium in the interior of $S \setminus \{q^*\}$, it follows from the Poincaré–Bendixson theorem that system (3) has at least a stable limit cycle which encircles q^*. ■

Remark 2. Suppose $\hat{h} < h < \min\{h_1, h_2\}$. If $m > r$, i.e. if harvesting rate of the prey is greater than intrinsic growth rate of the prey, then the origin is globally asymptotically stable and gradually the population density of both the species will decline and finally will tend to extinction and system (3) has not any limit cycles in $\mathbb{R}^2_+$.

3.4. Bifurcations of system (3)

In this section, we investigate the bifurcations that take place in system (3).

3.4.1. Transcritical bifurcation

When $m < r\left(1 - \frac{d}{ck}\right)$, the coexistence equilibrium p^* is a stable focus or node, while p_1 is an unstable saddle point. When $m = r\left(1 - \frac{d}{ck}\right)$, the two equilibria coincide and become $p_1 = p^* = (\frac{d}{c}, 0)$. Once $m < r\left(1 - \frac{d}{ck}\right)$, both equilibria exchange stability as p^* becomes an unstable saddle point and p_1 becomes a stable node. The system (3) undergoes a transcritical bifurcation involving the two equilibria p_1 and p^* at $m = r\left(1 - \frac{d}{ck}\right)$ (Figure 3). A transcritical bifurcation diagram is given in Figure 4.

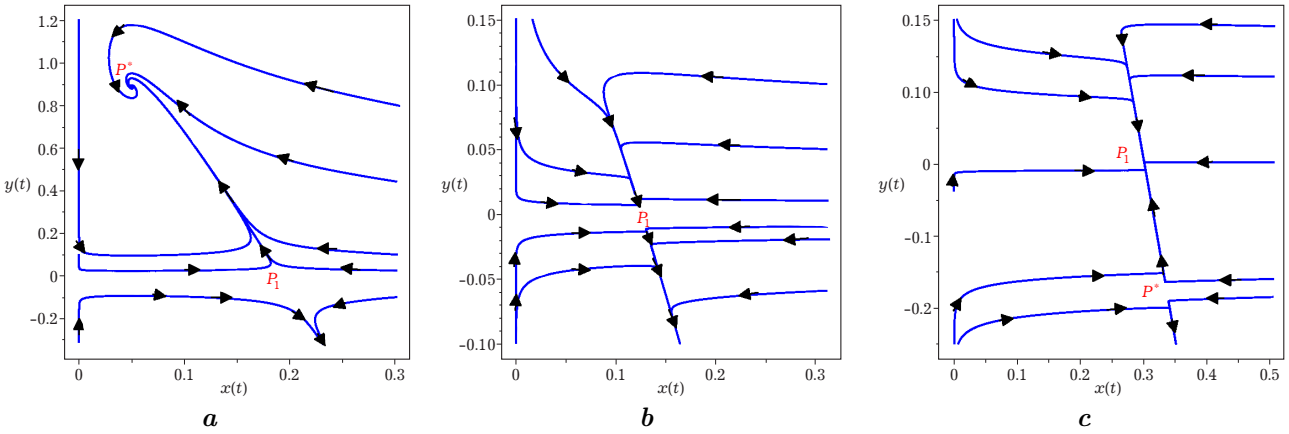

Fig. 3. The phase portrait of system (3), for $(\boldsymbol{a})$ $m < r(1 - \frac{d}{ck})$; $(\boldsymbol{b})$ $m = r(1 - \frac{d}{ck})$; $(\boldsymbol{c})$ $m > r(1 - \frac{d}{ck})$.

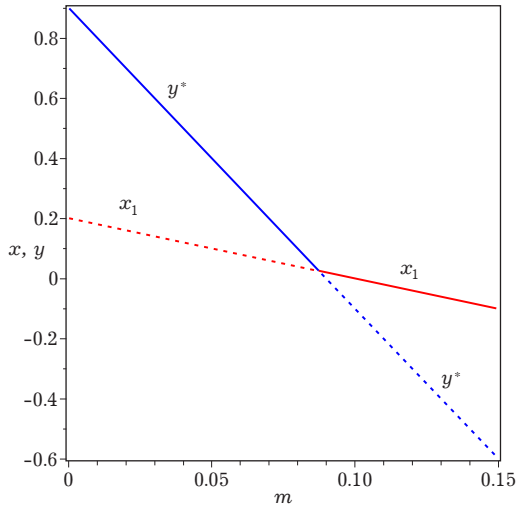

Fig. 4. The transcritical bifurcation diagram of x_1 and y^* versus m for system (3) with $r = 0.1$, $k = 0.2$, $a = 0.1$, $c = 0.5$ and $d = 0.01$. The red line with x_1 and blue line with y^* represents the curves of the prey and predator with equilibrium p_1 and p^*, respectively.

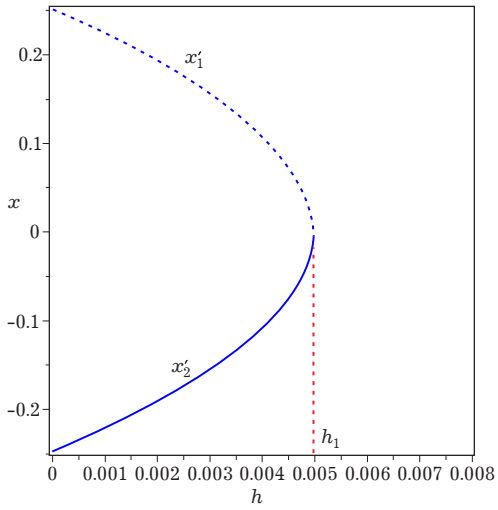

Fig. 5. The saddle-node bifurcation diagram of x_1' and x_2' versus h for system (3) with $r = 0.04$, $k = 0.5$, $a = 0.1$, $c = 0.07$, $d = 0.01$ and $h_1 = 0.005$. The dotted line with x_1' and solid line with x_2' represents the curves of the prey with equilibrium q_1 and q_2, respectively.

3.4.2. Saddle-node bifurcation

Suppose $h > h_2$. The number of equilibria of system (3) changes from zero to two. From Propositions 3 and 4, when $h > h_1$, there are no equilibrium points. When $h = h_1$, there is one equilibrium point q_0, that is a saddle-node. When $0 < h < h_1$, there are two equilibria q_1 and q_2 which are respectively, a saddle point and a node. Thus $h = h_1$ is a saddle-node bifurcation value (Figure 5).

3.4.3. Hopf bifurcation

The Hopf bifurcation is a very interesting type of bifurcations of systems. In this part, we analyze the existence of Hopf bifurcation in (3) at the coexistence equilibrium q^*.

Theorem 5. *When $h = \hat{h}$, system (3) exhibits a subcritical Hopf bifurcation at the equilibrium point q^*.*

Denote

$$\mathrm{V} = \left\{ (c, d, \bar{x}, h) \in \mathbb{R}^3_+ \colon \frac{d}{c} > \bar{x},\ h = \hat{h} < \min\{h_1, h_2\} \text{ and } \sigma > 0 \right\},$$

in order to show Theorem 5, we first prove the following proposition.

Proposition 6. If the parameter $(c, d, \bar{x}, h) \in \mathrm{V}$, then the equilibrium q^* of system (3) is an unstable weak focus of multiplicity one.

Proof. It follows from $h = \hat{h}$ that the positive equilibrium q^* of system (3) satisfies the trace $\tau_2 = 0$ and the determinant $\mathcal{D}_2 > 0$, then the Jacobian matrix $\mathfrak{J}_2(q^*)$ has a pair of pure imaginary eigenvalues. Hence, system (3) may undergo a Hopf bifurcation. We first shift the equilibrium point $q^* = (\hat{x}, \hat{y})$ to the origin using a change of coordinates $X = x - \hat{x}$ and $Y = y - \hat{y}$, we get

$$\begin{cases} \dot{X} = -\dfrac{ad}{c} Y - aXY - \dfrac{r}{k} X^2, \\ \dot{Y} = \left(\dfrac{cr}{a} - \dfrac{2rd}{ak} \right) X + cXY. \end{cases} \tag{12}$$

Then, we performed a suitable linear change of variables

$$\begin{cases} X = -\dfrac{1}{\left(\frac{cr}{a} - \frac{2rd}{ak}\right)} u, \\ Y = -\dfrac{1}{\sqrt{rd - \frac{2rd^2}{kc}}} v, \\ t = \dfrac{T}{\sqrt{rd - \frac{2rd^2}{kc}}} \end{cases} \tag{13}$$

we obtain

$$\begin{cases} u' = -v + a_{11} uv + a_{20} u^2, \\ v' = u + b_{11} uv, \end{cases} \tag{14}$$

where $u' = \frac{du}{dT}$, $v' = \frac{dv}{dT}$, $a_{11} = \frac{a}{rd - \frac{2rd^2}{kc}}$, $a_{20} = \frac{ra}{(ckr - 2rd)\sqrt{rd - \frac{2rd^2}{kc}}}$ and $b_{11} = \frac{-cak}{(ckr - 2rd)\sqrt{rd - \frac{2rd^2}{kc}}}$.

To determine the stability of the equilibrium q^*, we compute the Liapunov number σ for system (14) [26]. Moreover, if $\sigma \neq 0$, then a Hopf bifurcation exists.

We have,

$$\sigma = \frac{3\pi}{2} a_{11} a_{20} = \frac{3\pi r a^2}{2(ckr - 2rd)\sqrt{rd - \frac{2rd^2}{kc}}^3} > 0.$$

■

Proof of Theorem 5. From the Propositions 5 and 6, the equilibrium q^* is a hyperbolic unstable focus if $h \geqslant \hat{h}$; the equilibrium q^* is a hyperbolic stable focus if $0 < h < \hat{h}$. Hence, when parameter h passes through the bifurcation value $h = \hat{h}$ from one side of the surface V to the other side, system (3) undergoes a subcritical Hopf bifurcation and an unstable limit cycle appears in a neighborhood of q^* when $(c, d, \bar{x}) \in \mathrm{V}$ and $0 < h < \hat{h}$. ■

4. Numerical examples

In this section, we study the dynamics of system (3) numerically to verify the obtained analytic results.

Example 1. We take the parameter values as $r = 0.1$, $k = 0.2$, $a = 0.2$, $m = 0.01$, $c = 0.4$, $d = 0.01$ and $\bar{x} = 0.2$ in appropriate units. In this case, $p_0 = (0, 0)$ and $p_1 = (0, 0.18)$ are both saddle points and $p^* = (0.025, 0.387)$ is globally asymptotically stable (see Figure 6).

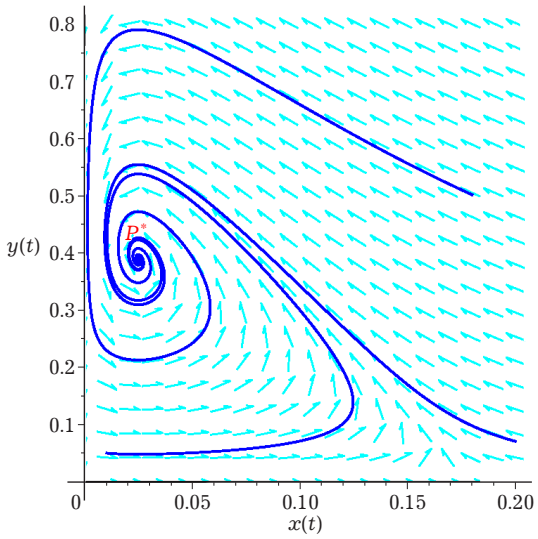

Fig. 6. The phase portrait of system (3) when p^* is globally asymptotically stable.

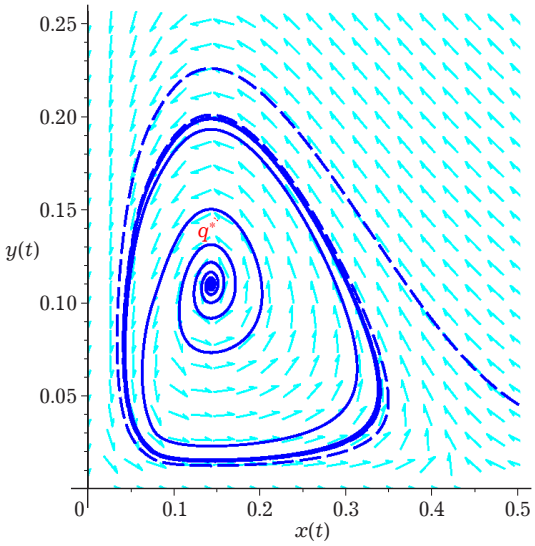

Fig. 7. A stable limit cycle of system (3) encircling the unstable equilibrium q^*.

Example 2. Using the following parameter values $r = 0.04$, $k = 0.5$, $a = 0.1$, $c = 0.07$, $d = 0.01$ and $m = 0.035$, we obtain $h_1 = 0.005$, $h_2 = 0.00408$ and $\hat{h} = 0.0016$. Selecting $\bar{x} = 0.05$, we get $h = 0.00175$. Thus $\hat{h} < h < \min\{h_1, h_2\}$ and $r > m$. System (3) has a stable limit cycle which encircles q^* (see Figure 7). The equilibria $p_0 = (0, 0)$ and $q_2 = (0.45, 0)$ are saddles and $q^* = (0.14, 0.16)$ is an unstable focus.

Example 3. Set $r = 0.2$, $k = 0.5$, $a = 0.1$, $c = 0.3$, $d = 0.01$ and $m = 0.1$, we obtain $h_1 = 0.025$, $h_2 = 0.0062$ and $\hat{h} = 0.00044$. Selecting $\bar{x} = 0.003$, we get $h = 0.0003$. Thus $h < \min\left\{h_1, h_2, \hat{h}\right\}$. The phase portrait of system (3) is shown in Figure 8. The equilibria $p_0 = (0, 0)$, $q_1 = (0.49, 0)$ are saddles and $q^* = (0.03, 1.77)$ is a stable focus.

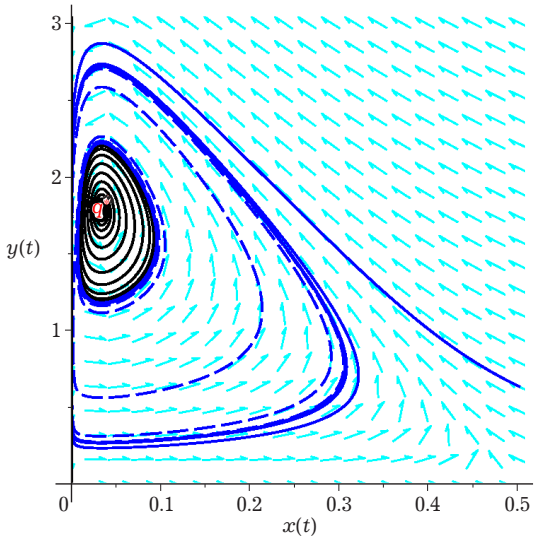

Fig. 8. Two limit cycles of system (3) encircling the stable equilibrium q^*.

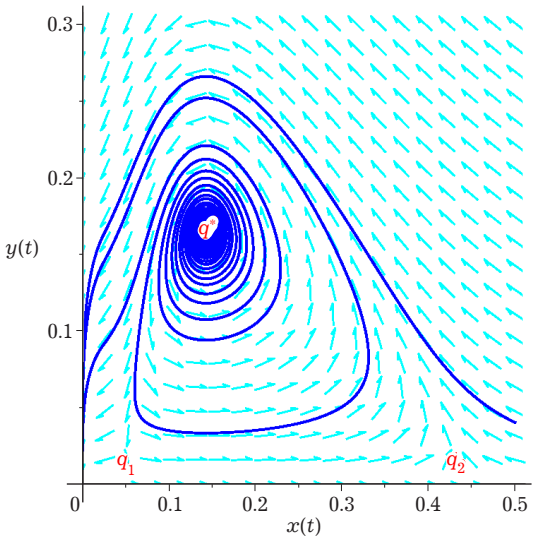

Fig. 9. The phase portrait of system (3) with globally asymptotically stable equilibrium p_0 and positive unstable equilibrium q^*.

We can see in this example that model (3) could exhibit more dynamical features: two limit cycles surrounding a positive equilibrium q^*, one stable and one unstable (see Figure 8). A trajectory (the dotted line) between the outside and inside periodic orbits ultimately tends to the outside periodic orbit, but a trajectory (the black line) starting from within the unstable periodic orbit finally tends to equilibrium q^*.

Example 4. If we take $r = 0.04$, $m = 0.07$, $k = 0.5$, $a = 0.1$, $d = 0.01$ and $c = 0.07$, we obtain $h_1 = 0.005$, $h_2 = 0.00408$ and $\hat{h} = 0.0016$. Choosing $\bar{x} = 0.025$, we get $h = 0.00175$. Thus $\hat{h} < h < \min\{h_1, h_2\}$ and $r < m$. The equilibria $p_0 = (0, 0)$ is globally asymptotically stable, $q_1 = (0.048, 0)$ and $q_2 = (0.45, 0)$ are both saddle points and $q^* = (0.14, 0.16)$ is an unstable focus. In this case, the population density of both the species tend to extinction (see Figure 9).

5. Conclusion

In this work, we have discussed the effects of non-smooth switched harvest on the prey for the predator–prey model (1). We have performed a qualitative analysis, thus examining the dynamics of the proposed model, and we have studied the existence and the global stability of the equilibrium. We have also shown the existence of at least one limit cycle when the harvesting rate of the prey is less than its growth rate and we have shown the existence of a second limit cycle numerically. We have shown that model (3) exhibits three bifurcations: a transcritical, a saddle-node, and a Hopf bifurcations. Finally, some numerical examples of the model are provided to illustrate the theoretical results.

Our model exhibits new dynamics compared to the existing harvesting models. We could show some differences for the model (3) with switched harvest on the prey and the model in [6] with switched harvest on the predator. We would like to simultaneously introduce the switched harvest in both prey and predator populations and add a superpredator to the model. The dynamics may be far richer and more complex, like the existence of a chaotic attractor [27].

Acknowledgment

The authors like to acknowledge the support of "Direction Générale de la Recherche Scientifique et du Développement Technologique DGRSDT. MESRS, Algeria".

[1] Berryman A. A. The origins and evolution of predator–prey theory. Ecology. **73** (5), 1530–1535 (1992).

[2] Hafdane M., Agmour I., El Foutayeni Y. Study of Hopf bifurcation of delayed tritrophic system: dinoflagellates, mussels, and crabs. Mathematical Modeling and Computing. **10** (1), 66–79 (2023).

[3] Kar T. K. Modelling and analysis of a harvested prey–predator system incorporating a prey refuge. Journal of Computational and Applied Mathematics. **185** (1), 19–33 (2006).

[4] Leard B., Lewis C., Rebaza J. Dynamics of ratio-dependent Predator–Prey models with nonconstant harvesting. Discrete and Continuous Dynamical Systems – S. **1** (2), 303–315 (2008).

[5] Lenzini P., Rebaza J. Nonconstant predator harvesting on ratio-dependent predator–prey models. Applied Mathematical Sciences. **4** (16), 791–803 (2010).

[6] Li B., Liu S., Cui J., Li J. A simple predator-prey population with rich dynamics. Applied Sciences. **6** (5), 151 (2016).

[7] Liu X., Huang Q. Comparison and analysis of two forms of harvesting functions in the two-prey and one-predator model. Journal of Inequalities and Applications. **2019**, 307 (2019).

[8] Lv Y., Yuan R., Pei Y. Two types of predator–prey models with harvesting: Non-smooth and non-continuous. Journal of Computational and Applied Mathematics. **250**, 122–142 (2013).

[9] Xiao M., Cao J. Hopf bifurcation and non-hyperbolic equilibrium in a ratio-dependent predator-prey model with linear harvesting rate: Analysis and computation. Mathematical and Computer Modelling. **50** (3–4), 360–379 (2009).

[10] Xiao D., Jennings L. S. Bifurcations of a ratio-dependent predator–prey system with constant rate harvesting. SIAM Journal on Applied Mathematics. **65** (3), 737–753 (2005).

[11] Xiao D., Li W., Han M. Dynamics in a ratio-dependent predator-prey model with predator harvesting. Journal of Mathematical Analysis and Applications. **324** (1), 14–29 (2006).

[12] Zhang Y., Zhang Q. Dynamic behavior in a delayed stage-structured population model with stochastic fluctuation and harvesting. Nonlinear Dynamics. **66** (1), 231–245 (2011).

[13] Seo G., Kot M. A comparison of two predator-prey models with Holling's type I functional response. Mathematical Biosciences. **212** (2), 161–179 (2008).

[14] Ang T. K., Safuan H. M., Kavikumar J. The impact of harvesting activities on prey–predator fishery model in the presence of toxin. Jounal of Science and Technology. **10** (2), 128–135 (2018).

[15] Chauhan S., Bhatia S. K., Chaudhary P. Effect of pollution on prey–predator system with infected predator. Communication in Mathematical Biology and Neuroscience. 14 (2017).

[16] Kumar U., Mandal P. S. Role of Allee effect on prey–predator model with component Allee effect for predator reproduction. Mathematics and Computers in Simulation. **193**, 623–665 (2022).

[17] Zhang H., Cai Y., Fu S., Wang W. Impact of the fear effect in a prey–predator model incorporating a prey refuge. Applied Mathematics and Computation. **356**, 328–337 (2019).

[18] Bohn J., Rebaza J., Speer K. Continuous threshold prey harvesting in predator–prey models. International Journal of Mathematical and Computational Sciences. **5** (7), 996–1003 (2011).

[19] Su J. Degenerate Hopf bifurcation in a Leslie–Gower predator–prey model with predator harvest. Advances in Difference Equations. **2020**, 194 (2020).

[20] Dai G., Tang M. Coexistence region and global dynamics of a harvested predator–prey system. Journal on Applied Mathematics. **58** (1), 193–210 (1998).

[21] Haque M., Sarwardi S. Effect of toxicity on a harvested fishery model. Modeling Earth Systems and Environment. **2** (3), 122 (2016).

[22] Vijayalakshmi T., Senthamarai R. Study of two species prey–predator model in imprecise environment with harvesting scenario. Mathematical Modeling and Computing. **9** (2), 385–398 (2022).

[23] Birkoff G., Rota G. C. Ordinary differential equations. New York, Wiley (1978).

[24] Hale J. K., Lunel S. M. V. Introduction to Functional Differential Equations. Springer Science and Business Media (2013).

[25] Dumortier F., Llibre J., Artés J. C. Qualitative theory of planar differential systems. Berlin, Springer (2006).

[26] Perko L. Differential equations and dynamical systems. Springer–Verlag (2000).

[27] Rasedee A. F. N., Abdul Sathar M. H., Mohd Najib N., Wong T. J., Koo L. F. Numerical analysis on chaos attractors using a backward difference formulation. Mathematical Modeling and Computing. **9** (4), 898–908 (2022).

Динамічна поведінка моделі "хижак–жертва" з неплавним здобуванням жертви

Мезіані Т., Мохдеб Н.

Лабораторія прикладної математики, Факультет точних наук, Університет Беджайя, Алжир

Метою цієї роботи є дослідження динаміки нової моделі "хижак–жертва", де вид жертви підкоряється закону логістичного зростання та піддається негладкому перемиканню здобичі: коли щільність жертви нижча значення перемикання – швидкість здобування жертви є лінійною, в іншому випадку – швидкість здобування постійна. Описано рівноваги запропонованої системи та досліджено обмеженість її розв'язків. Обговорюється існування періодичних розв'язків, показано появу двох граничних циклів: нестійкого внутрішнього граничного циклу та стійкого зовнішнього. Оскільки значення параметрів змінюються, для моделі виявляється декілька видів біфуркацій, таких як транскритична, сідло–вузлова та Хопфа. Накінець для підтвердження отриманих теоретичних результатів подано декілька чисельних прикладів моделі.

Ключові слова: *модель "хижак–жертва"; перемикання здобування; стійкість; біфуркація; граничний цикл.*